

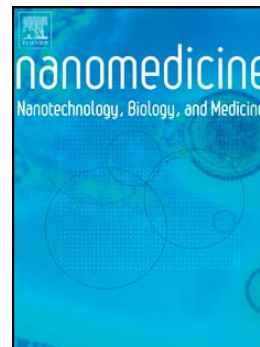
This is the Post-print version of the following article: *Alejandro Ramirez-Lee Manuel, Pedro Pablo Martinez-Cuevas, Hector Rosas-Hernandez, Cuauhtémoc Oros-Ovalle, Mariela Bravo-Sanchez, Gabriel Alejandro Martinez-Castañon, Carmen Gonzalez, Evaluation of vascular tone and cardiac contractility in response to silver nanoparticles, using Langendorff rat heart preparation, Nanomedicine: Nanotechnology, Biology and Medicine, Volume 13, Issue 4, 2017, Pages 1507-1518*, which has been published in final form at: <https://doi.org/10.1016/j.nano.2017.01.017>

© 2017. This manuscript version is made available under the Creative Commons Attribution-NonCommercial-NoDerivatives 4.0 International (CC BY-NC-ND 4.0) license <http://creativecommons.org/licenses/by-nc-nd/4.0/>

Accepted Manuscript

Evaluation of vascular tone and cardiac contractility in response to silver nanoparticles, using Langendorff rat heart preparation

Ramirez-Lee Manuel Alejandro, Martinez-Cuevas Pedro Pablo, Rosas-Hernandez Hector, Oros-Ovalle Cuauhtémoc, Bravo-Sanchez Mariela, Martinez-Castañon Gabriel Alejandro, Gonzalez Carmen



PII: S1549-9634(17)30024-2
DOI: doi: [10.1016/j.nano.2017.01.017](https://doi.org/10.1016/j.nano.2017.01.017)
Reference: NANO 1525

To appear in: *Nanomedicine: Nanotechnology, Biology, and Medicine*

Received date: 13 October 2016
Revised date: 24 January 2017
Accepted date: 30 January 2017

Please cite this article as: Alejandro Ramirez-Lee Manuel, Pablo Martinez-Cuevas Pedro, Hector Rosas-Hernandez, Cuauhtémoc Oros-Ovalle, Mariela Bravo-Sanchez, Alejandro Martinez-Castañon Gabriel, Carmen Gonzalez, Evaluation of vascular tone and cardiac contractility in response to silver nanoparticles, using Langendorff rat heart preparation, *Nanomedicine: Nanotechnology, Biology, and Medicine* (2017), doi: [10.1016/j.nano.2017.01.017](https://doi.org/10.1016/j.nano.2017.01.017)

This is a PDF file of an unedited manuscript that has been accepted for publication. As a service to our customers we are providing this early version of the manuscript. The manuscript will undergo copyediting, typesetting, and review of the resulting proof before it is published in its final form. Please note that during the production process errors may be discovered which could affect the content, and all legal disclaimers that apply to the journal pertain.

TITLE PAGE

Evaluation of vascular tone and cardiac contractility in response to silver nanoparticles, using Langendorff rat heart preparation.

Ramirez-Lee Manuel Alejandro^a, Martinez-Cuevas Pedro Pablo^a, Rosas-Hernandez Hector^a, Oros-Ovalle Cuauhtémoc^b, Bravo-Sanchez Mariela^c, Martinez-Castañon Gabriel Alejandro^d, Gonzalez Carmen^a.

^aFacultad de Ciencias Químicas, Universidad Autónoma de San Luis Potosí, Av. Manuel Nava Num. 6, Col. Universitaria, 78210 San Luis Potosí, S.L.P., Mexico.

^bDepartamento de Patología, Hospital Central «Dr. Ignacio Morones Prieto», Av. Venustiano Carranza Num. 2395, Col. Universitaria, 78210 San Luis Potosí, S.L.P., Mexico.

^cInstituto Potosino de Investigación Científica y Tecnológica, División de Materiales Avanzados, Camino a La Presa de San José 2055, Lomas 4 sección, 78216 San Luis Potosí, S.L.P., Mexico.

^dFacultad de Estomatología, Universidad Autónoma de San Luis Potosí, Av. Manuel Nava Num. 2, Col. Universitaria, 78290 San Luis Potosí, S.L.P., Mexico.

Corresponding author: Carmen Gonzalez, Ph. D.

Address: Facultad de Ciencias Químicas, Universidad Autónoma de San Luis Potosí, Av. Manuel Nava Num. 6., Col. Universitaria. Zip Code 78210, San Luis Potosí, Mexico.

Phone: +52-444-0262440 x 6459

E-mail: cgonzalez.uaslp@gmail.com; gonzalez.castillocarmen@fcq.uaslp.mx

Conflict of interest: There are no conflicts of interests.

This work was supported by Consejo Nacional de Ciencia y Tecnologia through the fellowships of Ramirez-Lee (318669), Martinez-Cuevas (318780), Rosas-Hernandez (317768) and the grants C15-FAI-04-33.33; C15-PIFI-06-02.02 and C16-PIFI-09-08.08. We also thanks LINAN for providing access to XPS facilities.

Word count for abstract: 149

Word count for complete manuscript: 4986

Number of references: 60

Number of figures: 7

Number of tables: 0 (zero)

Number of supplementary online-only files: 1

ABSTRACT

Silver nanoparticles (AgNPs) have been widely used because of their antimicrobial properties. However, several reports suggest that AgNPs exposure promote cardiac effects that involve nitric oxide (NO) and oxidative stress (OS). Nevertheless, there are no studies related to AgNPs-induced effects in cardiac physiology. The aim of this study was to evaluate the AgNPs direct actions on coronary vascular tone and cardiac contractility using Langendorff rat heart preparation. Low concentrations of AgNPs (0.1 and 1 $\mu\text{g}/\text{mL}$) increased NO derived from inducible NO-synthase (iNOS), without modifying cardiac parameters. Meanwhile, high concentrations (10 and 100 $\mu\text{g}/\text{mL}$) promoted a sustained vasoconstriction and increased cardiac contractility related to OS, leading to rhabdomyolysis. Furthermore, AgNPs were internalized in the cardiac muscle, hindering classic actions induced by phenylephrine (Phe) and acetylcholine (ACh). These data suggest that AgNPs affect cardiac physiology in function of the concentration and in part of the NO generation, NOS expression and OS.

Keywords: Silver nanoparticles; coronary vascular tone; myocardial contractility; nitric oxide; oxidative stress.

Abbreviations: ACh, Acetylcholine; AgBMs, Silver bulk materials; AgNO_3 , Silver nitrate; AgNPs, Silver nanoparticles; CAT, Catalase; CEC, Rat coronary endothelial cells; CVS, Cardiovascular system; DLS, Dynamic light scattering; eNOS, Endothelial nitric oxide synthase; GAPDH, Glyceraldehydes-3-phosphate dehydrogenase; iNOS, Inducible nitric oxide synthase; LVP, Left ventricle pressure; MDA, Malondialdehyde; NMs, Nanomaterials; nNOS, Neuronal nitric oxide synthase; NO, Nitric oxide; NO_2 , Nitrites; NO_3 , Nitrates; NPs, Nanoparticles; O_2^- , Superoxide anion; OS, Oxidative stress; Phe, Phenylephrine; PIE, Positive inotropic effect; PP, Perfusion pressure; ROS, Reactive oxygen species; SEM, Scanning electron microscopy; SOD,

Superoxide dismutase; SVSC, Shirley-Vegh-Salvi-Castle; TEM, Transmission electron microscopy; VIP, Vacuum Infiltration Processor; XPS, X-ray photoelectron spectroscopy.

ACCEPTED MANUSCRIPT

BACKGROUND

Lately, nanotechnology industry has led to the development of nanomaterials (NMs), which are structures with novel and unique physicochemical properties attributable to their size (1 to 100 nm) (1). However, their toxic or protective effects in biological systems are not fully studied. Silver nanoparticles (AgNPs) are the most common NMs used as effective antimicrobial agents in an increasing number of products (2). Approximately, 14% of the AgNPs-containing products could release these NPs through their manipulation, representing a potential source of exposure (2, 3). Several reports have shown that AgNPs are able to translocate, enter into the human body through different routes of exposure (3) and distribute to major organs through the blood stream, including the heart (3, 4). Epidemiological studies have demonstrated that NPs exposure promote negative effects on cardiovascular system (CVS), including cardiac dysfunction, dysrhythmia, heart failure and myocardial infarction (5). However, there is limited information about AgNPs effects in cardiac function; which is regulated by nitric oxide (NO), a free radical synthesized enzymatically by endothelial NO-synthase (eNOS), neuronal (nNOS) and inducible (iNOS) synthases (6). NO acting on heart is produced by all cell types composing the myocardium, like the endothelium, a specialized epithelium that coats blood vessels lumen (7). In this concern, it has been reported that 35.75 nm AgNPs at high concentrations ($>100 \mu\text{g/mL}$), stimulate proliferation of rat coronary endothelial cells (CEC) related to eNOS-derived NO and induced a NO-dependent vasodilation, in similar fashion to acetylcholine (ACh), on Wistar rat aorta rings (8). Likewise, *in vivo* studies reported that exposure of Ross broiler chickens (9) and zebrafish embryos (10) to 5-20 nm AgNPs (>50 to $100 \mu\text{g/mL}$), decrease heart rate and cardiac contractility, indicating that they could interfere directly with cardiac muscle activity. Also, it was demonstrated that 35.75 nm AgNPs ($<5 \mu\text{g/mL}$) induced an endothelium-dependent

vasoconstriction in Wistar rat aorta rings, in absence and presence of phenylephrine (Phe) (8), a very well-known vasoconstrictor agent (11); suggesting that AgNPs may induce dual actions in vascular and cardiac function involving eNOS-derived NO. However, another report indicated that inhalation exposure of Sprague Dawley rats to 33 and 39 nm AgNPs (100 and 1000 $\mu\text{g}/\text{m}^3$) do not affect vascular nor cardiac function, since no modifications to vascular tone, heart rate nor left ventricular systolic pressure were detected (12), evidencing their controversial actions in all these approaches. On the other hand, exposing guinea pigs dermally to 100 nm AgNPs during 13 weeks, cardiotoxicity was observed as cardiomyocytes deformities, inflammation and congestion (13). In this regard, *in vivo* and *in vitro* studies have suggested that AgNPs cardiotoxicity may imply oxidative stress (OS) (14), either by reducing activity of antioxidant enzymes such as superoxide dismutase (SOD) and catalase (CAT) (15), or promoting reactive oxygen species (ROS) generation (16). Nevertheless, there are no reports exclusively focused on AgNPs actions upon cardiac physiology using an integrative model. Recently, the isolated Langendorff heart preparation has been proposed for the assessment of NMs effects in CVS (4, 17, 18). The aim of this study was to evaluate the effects of AgNPs on cardiac contractility and coronary vessels tone using isolated perfused rat hearts, conjointly with their association with NO, NOS expression and OS generation.

METHODS

Synthesis of silver nanoparticles

AgNPs were synthesized from a 100 mL of 0.01 M AgNO_3 deionized water-based solution, placed in 1 L reaction vessel. Ten mL of 1% (w/v) gallic acid solution were mixed with 100 mL of Ag^+ solution using constant magnetic stirring. Then, the pH value of the solution was immediately adjusted (pH=11) with NaOH 1.0 M. Thereafter, each AgNPs suspension was

flocculated changing the pH to 1.5 using nitric acid; the resulted suspension was filtered with a nitrocellulose filter (Millipore, 0.1 μm pore diameter) in a vacuum filter flask (Nalgene). AgNPs on the filter were washed several times with deionized water until neutral pH. Finally, AgNPs were dispersed in deionized water and diluted to a metered volume to reach a concentration of 1017 $\mu\text{g/mL}$, which was confirmed with atomic absorption analysis (19).

Silver nanoparticles and silver bulk materials characterization

AgNPs size and zeta potential was determined using dynamic light scattering (DLS) assay, using a DLS Malvern Zetasizer Nano ZS (Instruments Worcestershire, United Kingdom). NPs shape was confirmed by transmission electron microscopy (TEM) analysis, using a JEOL JEM-1230 microscope. Morphology and size of silver bulk materials (AgBMs) were observed using a scanning electron microscope (SEM, JOEL JSM-1650). X-ray photoelectron spectroscopy (XPS) was conducted in a PHI 5000 VersaProbe II system (Physical Eletronics, USA) equipped with a monochromated Al-K α X-ray source. As AgNPs are suspended in liquid solution, these were prepared by solvent evaporation method (20) at room temperature over silicon wafers previously cleaned. Also 99.99% silver foil (Alfa Aesar, USA) was analyzed under the same conditions to use as reference sample. Binding energies were calibrated by setting the binding energy of adventitious C 1s to 284.8 eV. XPS spectra were fitted using the Double Lorentzian line shape (21) to model the asymmetry in metallic gold and in the case when oxide states where found was used the Voigt function. The background was removed using Shirley-Vegh-Salvi-Castle (SVSC) background (22).

Animals

Male Wistar rats (250-300 g) were used in all experiments. Rats were housed in clear plastic containers under a 12-h dark/light cycle with *ad libitum* access to water and food. All procedures

were performed in accordance with the National Institute of Health Guide for the Use and Care of Laboratory Animals guidelines and approved by the Animal Care and Use Committee from the Faculty of Chemistry of the University of San Luis Potosi, Mexico (protocol number CEID2014032).

Isolated Langendorff heart preparation

In vitro retrograde heart perfusion was performed at constant flow-rate mode (23, 24). Briefly, under anesthesia with sodium pentobarbital (50 mg/kg ip) heart was rapidly excised and transferred to ice-cold Krebs solution containing (mM): NaCl 117.8, NaHCO₃ 24.2, KCl 6.0, MgSO₄ 1.2, NaH₂PO₄ 1.2, glucose 5.0, CaCl₂ 1.75 and pyruvate 5.0. Then, heart was connected to an aortic cannula of Langendorff apparatus and perfused at constant flow-rate (8 mL/min) with Krebs solution which was constantly bubbled with 95% O₂ and 5% CO₂ at 37 °C. A deionized water-filled latex balloon connected to a pressure transducer was inserted through the mitral valve into the left ventricle to allow isovolumetric contractions and continuously record the left ventricle pressure (LVP) as an index of cardiac contractility. Another pressure transducer located above the aorta recorded the perfusion pressure (PP), considered as an index of coronary vascular tone. Two wire electrodes were placed in the right atrium and apex to maintain heart rate at 4.5 beats per second. Haemodynamic parameters were acquired and analyzed using HSE-ISOHEART W software from Harvard Apparatus (Holliston, MA, USA).

Treatments

After preparation, a 20 min stabilization phase was allowed prior to treatments. To corroborate tissue functionality, Phe and ACh (10 µM) were perfused at the beginning and end of each experiment. Increasing concentrations (0.1, 1, 10 and 100 µg/mL) of AgNPs were perfused and the effects were evaluated by PP and LVP. Micro-sized Ag particles, AgBMs and AgNO₃ (0.1, 1,

10 and 100 $\mu\text{g/mL}$) were also perfused as control of size and ionic silver, respectively. All treatments were injected as bolus. At the end of the experiment, hearts were sectioned in two slices from apex to base. One section was used for determine protein expression and the other one for lipid peroxidation.

Western blot analysis

Protein expression was evaluated in cardiac tissue using western blot (25).

Nitric oxide production

NO production was quantified indirectly by measuring nitrites (NO_2) and nitrates (NO_3) (26), using the Griess method (27).

Malondialdehyde generation

Malondialdehyde (MDA) was measured as an index of lipid peroxidation, determined by thiobarbituric acid assay as previously described (28).

Histological study

Separately, treated hearts with AgNPs were fixed in 10% paraformaldehyde-PBS for 24 h. Samples were processed with automated Tissue-Tek Vacuum Infiltration Processor (VIP) five (Sakura, Zoeterwoude, The Netherlands). VIP program started with dehydration process by sequential steps in 70%, 96% and 100% ethanol, and followed by three baths of xylene before the process finished with paraffin (Paraplast®) embedding. 3 μm paraffin sections were mounted on saline-coated slides and with nuclear fast red-aluminum solution (Merck, Darmstad, Germany). Images were acquired using an Olympus CX41 microscope (400x and 1000x objective) and a conventional CCD camera (Infinity 1, Lumenera) (29). Qualitative determination of silver presence in cardiac tissue was performed by Grimelius stain. 3 μm slides were immersed in distilled water for 1 min, incubated in silver solution (1% AgNO_3 with 0.2 M

sodium acetate and 0.2 M acetic acid) at 60 °C for 3 h. Then, dipped in reducing solution (5% sodium sulfate with 1% hydroquinone) at 45 °C for 1 h. After a final washout with distilled water, slides were analyzed (30).

Statistical analysis

Results were expressed as mean \pm SEM. After confirmation of data normality by the Shapiro-Wilk normality test, a one-way analysis of variance (ANOVA) was used to compare values between groups followed by Fisher Least Significant Differences (LSD) post hoc test. Kruskal-Wallis nonparametric test followed by Bonferroni-corrected Mann-Whitney U post hoc test was used to compare non-normal data groups.

RESULTS

Physical characterization of AgNPs

TEM analysis revealed that AgNPs have pseudo-spherical shapes (Fig.1 A). SEM analysis showed AgBMs having irregular shape in micrometers order (Fig.1 B). DLS analysis indicated that AgNPs have a mean particle size of 15 ± 4 nm (ranging from 8.75 to 37.5 nm) (Fig.1 C). The zeta potential of AgNPs stock suspension was -58.2 ± 5.15 mV, confirming its high stability, since particles with zeta potential values more positive than +30 mV or more negative than -30 mV are considered as stable (31). For AgNPs (Fig.2 A), XPS spectrum shows two separate peaks having binding energies of 367.5 and 373.5 eV corresponding to Ag ($3d_{5/2}$) and Ag ($3d_{3/2}$) transitions, respectively, likewise to those observed in the reference sample Ag foil (Fig.2 B). Characteristic spin-orbit separation of 6 eV and ratio of 0.75 between 5/2 and 3/2 branches is present in the spectra. Characteristic loss features of metallic Ag are seen at higher binding energy side of each spin-orbit component in both cases. The FWHM value was found to be 0.73 and 0.75 eV for AgNPs and the reference, respectively. Further evidence that there are not any oxidation state in

the sample AgNPs is the comparison of our spectra with standard spectrum in XPS Handbook (32) which data is available for analysis in Multipak software v9.0 (Physical Electronics, USA). For this spectrum, the FWHM value is 0.72 (Fig.2 C).

AgNPs modify vascular coronary tone and cardiac contractility

Isolated perfused rat hearts were exposed to increasing concentrations of AgNPs (0.1, 1, 10 and 100 $\mu\text{g}/\text{mL}$) to evaluate their effects. Cardiac functionality was first tested using contractile and dilator controls, Phe and ACh (10 μM), respectively (Fig.3 A and B). After these agents induced their classic actions, PP and LVP values returned to baseline. We observed in representative trace recordings that, low concentrations of AgNPs (0.1 and 1 $\mu\text{g}/\text{mL}$) induced a non-significant decrease in PP (Fig.3 C and E) and LVP (Fig.3 D and F). Nevertheless, high concentrations of AgNPs (10 and 100 $\mu\text{g}/\text{mL}$) stimulated vasoconstriction and cardiac contractility, i.e., a positive inotropic effect (PIE), since both PP and LVP values increased, but did not return to the baseline (Fig.3 C to F). We also found that the classic effects of Phe (contractile) (33) and ACh (dilator) (34), were not observed after AgNPs treatment (Fig.3 C and D), suggesting that these NMs could modify the responses induced by these vasoactive agents.

AgNPs increase iNOS-derived NO production and oxidative stress in cardiac tissue

Since NO participates on cardiac physiology regulation (6), we quantified its production in venous effluent from perfused rat hearts. As expected, only ACh, a very well-known NO-dependent dilator agent (35), increased NO production before AgNPs exposure, meanwhile Phe did not modify it (Fig.4 A). Otherwise, only low concentrations of AgNPs (0.1 and 1 $\mu\text{g}/\text{mL}$) increased NO generation compared to control. Interestingly, ACh did not increase NO after AgNPs treatment (Fig.4 A), suggesting that AgNPs may influence ACh-induced NO-dependent dilator effect on isolated hearts. On the other hand, considering that AgNPs can induce OS in the

heart (15, 16), we evaluated MDA generation, as an OS marker. We found that only high concentrations of AgNPs (10 and 100 $\mu\text{g}/\text{mL}$) increased MDA levels compared to control (Fig.4 B), suggesting that OS may play a role in the contractile effect induced by AgNPs in this model. In view of the pattern of AgNPs-induced effects upon PP, LVP, NO and MDA generation, we evaluated eNOS, iNOS, CAT and SOD expression as a possible part of the molecules involved in the mechanism of action. Western blot analysis showed that AgNPs did not modify eNOS, CAT nor SOD expression. However, AgNPs at 0.1 and 1 $\mu\text{g}/\text{mL}$ significantly increased the expression of iNOS compared to control (Fig.4 C and D), indicating that this NOS isoform may be involved in AgNPs-induced NO generation, even when no physiological changes were detected, it also suggest a damage at the tissue level.

***In situ* cardiac effects and location of AgNPs**

To gain a deeper insight into the AgNPs effects, cardiac tissue was prepared for histology. Under control conditions, except for edema, no changes were detected (Fig.5 A and F). However, in AgNPs 0.1 $\mu\text{g}/\text{mL}$ treated hearts, cell tumefaction, vacuoles around the nucleus and cytosol, nucleus and myofibrillar degeneration were observed, but preserving muscle striations (Fig.5 B and G). Furthermore, AgNPs 1 $\mu\text{g}/\text{mL}$ induced cell atrophy, slightly loss of transversal striations, tumefaction, myofibrillar and nucleus degeneration (Fig.5 C and H). Meanwhile, 10 and 100 $\mu\text{g}/\text{mL}$ AgNPs promoted severe damage, evidenced by cellular vacuolization, edema, sarcoplasmic retractions, degradation and fragmentation of nucleus, karyorrhexis, necrosis, myofibrillar separation and degradation indicative of rhabdomyolysis (Fig.5 D, E, I and J). AgNPs 100 $\mu\text{g}/\text{mL}$ showed the highest injury rate. These results suggest AgNPs cardiac-induced damage it intensifies as the concentration increases.

AgNPs are able to translocate within the cardiac tissue

Grimelius technique was used to detect silver in heart after AgNPs treatment. We did not find silver under control conditions (Fig.5 K). However, we detected microscopic silver clusters only in the cardiac tissue treated with 100 µg/mL AgNPs (Fig.5 M), using the tissue from appendix carcinoid tumor as a positive control reference (Fig.5 L). Silver clusters are located within the myocardium, specifically in the sarcoplasm, suggesting that AgNPs may cross the coronary capillaries and the cardiac muscle sarcolemma. There were no silver clusters detected inside the endothelium nor blood vessels (Fig.5 M).

AgNPs-induced cardiac effects are attributable to their size

To investigate particle size and ionic processes influence on AgNPs effects, rat hearts were exposed to increasing concentrations (0.1, 1, 10 and 100 µg/mL) of AgBMs and AgNO₃. Results showed that AgBMs (Fig.6 A and C) nor AgNO₃ (Fig.6 B and D) did not modify cardiac physiological parameters. Additionally, AgBMs did not change the NO production in comparison with control (Fig.6 E), but AgNO₃ increased NO levels at the same concentrations (0.1 and 1 µg/mL) (Fig.6 F) that AgNPs did. Interestingly, ACh-induced NO production nor Phe and ACh actions were not observed after AgBMs and AgNO₃ treatments. These data suggest that at least the AgNPs-induced effects on cardiac physiology may be due to their nanometer size; however ionic Ag may not be involved in cardiac effects, but it could be involved in NO production stimulation.

AgBMs and AgNO₃ do not induce oxidative stress nor modify protein expression in cardiac tissue

Furthermore, we evaluated the MDA generation and eNOS, iNOS, CAT and SOD expression in cardiac tissue after treatment with AgBMs and AgNO₃ cumulative concentrations (0.1-100

$\mu\text{g/mL}$). MDA generation (Fig.7 A) nor protein expression (Fig.7 B and C) were not modified after these treatments, suggesting that AgNPs responses under the evaluated parameters, depend on their size and own nature.

DISCUSSION

In this study we investigated the direct actions of AgNPs on cardiac physiology using the isolated perfused rat heart Langendorff preparation, and their association with NO, NOS and OS as possible mediators. The major finding was that AgNPs modified coronary vascular tone and myocardial contractility associated to NO generation and OS, as well as the loss effects of vasoactive controls Phe and ACh after AgNPs treatment. Physical characterization revealed that AgNPs exhibit a narrow size distribution and to be stable in suspension. According to the Ag standard spectrum from XPS Handbook (32) and the Ag foil reference sample, the resulting peaks for AgNPs spectra corresponds to Ag ($3d_{5/2}$) and Ag ($3d_{3/2}$) photoelectrons, confirming that pure Ag is present in AgNPs synthesized with gallic acid. Likewise, it has been reported using XPS that gallic acid-synthesized AgNPs were found to be composed of pure Ag without signs of oxidations (36). Therefore, we suggest that AgNPs under evaluation are essentially of pure Ag with no impurities nor oxidation processes. On the other hand, a recent report indicated that AgNPs exposure at concentrations high concentrations ($>95 \mu\text{g/mL}$) for prolonged periods, can cause high blood pressure (37). In concordance, our data showed that AgNPs 10 and 100 $\mu\text{g/mL}$ promoted vasoconstriction and PIE; however, no generation of NO was detected, only physiological events were associated to NO at AgNPs low concentrations. It is known, as about vascular tone, while NO low concentrations increase myocardial contractility, high concentrations exert a negative inotropic effect (38). In this regard, it has been demonstrated that AgNPs induce an endothelium- and NO-dependent vasodilation on Wistar rat aortic rings.

Furthermore, the same study reported on CEC, that AgNPs are able to activate eNOS and the subsequent generation of NO (8). Here we found that AgNPs do not change the eNOS expression at the concentrations where NO production was observed, but instead, it increased iNOS expression, which is also a NOS isoform that can produce NO acting on heart (6). Furthermore, we believe that the effects induced by low concentrations of AgNPs were not statistically different because, as histological analysis revealed, NPs induced abnormalities on cardiac muscle, such as myofibrillar and nucleus degeneration, cellular tumefaction and slight loss of muscle striations, that could result in cardiac contractile machinery impairment, impacting the mechanism of relaxation and affecting the proper functionality of the heart in response to any agent (39). Moreover, these differences may also be explained because AgNPs used in the mentioned study, have bigger size (35.75 ± 13.1 nm) compared to NPs we employed (15 ± 4 nm). Also, their synthesis methods were different, and considering that is well accepted, among size and coating, synthesis method strongly influence AgNPs biological effects (40), we certainly do not discard the involvement of target organ or even species utilized in these experimental approaches. On the other hand, we showed that high concentrations of AgNPs induced vasoconstriction and PIE, without modifying NO levels, eNOS nor iNOS expression. In spite of it has been demonstrated that reduction of NOS-derived NO release, induce PIE in rat heart (41), and also that elevated contractility is a result of iNOS inhibition in dog heart (42), we suggest that at least in this model NO, is not involved in the effects induced by AgNPs at 10 and 100 $\mu\text{g/mL}$, since instead they increased MDA levels, without modifying SOD and CAT expression. One possible explanation for these effects is that, ROS-induced lipid peroxidation promotes MDA formation (43), that in turn increase the activity but not expression (44) of SOD and CAT in order to counteract the ROS damage (45). Several reports have indicated that OS is an

important factor in AgNPs-induced effects (46), for instance, AgNPs-induced genotoxicity and cytotoxicity on heart cells from *Catla catla* fish are associated with an increase in lipid peroxidation and reduced SOD and CAT activity (15). In fact, and in concordance with our results, dietary exposed Wistar rats to AgNPs elevated MDA levels in cardiac tissue without modifying the SOD and CAT activity (47). Likewise, orally exposure of Sprague-Dawley rats to AgNPs stimulated the cardiac generation of superoxide anion ($O_2^{\cdot-}$) without altering SOD activity (16), suggesting that in our study, even when their expression was not modified, SOD and CAT activity may not be altered by AgNPs. Interestingly, $O_2^{\cdot-}$, the first generated ROS (45), is also considered as a contractile agent (48), which suggests that AgNPs-induced vasoconstriction and PIE at high concentrations could be mediated partially through OS. Supporting our hypothesis, histological analysis showed that high concentrations of AgNPs induced rhabdomyolysis, described as the disintegration of striated muscle (49), which mechanism is a result of an injury caused directly by trauma, toxins, drugs, among others, leading to $2Na^+/Ca^{2+}$ exchanger activation resulting in an excessive Ca^{2+} intracellular concentration (50). High Ca^{2+} levels triggers simultaneously, ROS-induced lipid peroxidation and sustained myofibrillar contraction that further depletes ATP (51). Consequently, as ending result, self-sustaining myolytic cascade causes massive necrosis of cardiac muscle releasing its content to extracellular space and bloodstream (52). Another important finding, it was that Phe-induced contractile and ACh-induced NO-dependent dilator effects were not observed after AgNPs treatment. In cardiomyocytes, it has been reported that AgNPs bind to β_2 -adrenergic receptors in localized and specific domains (53); considering that Phe primarily binds to α_1 adrenergic receptor to induce contractile effects, but also have affinity to β_2 receptors, promoting a transient vasodilator activity (54), we hypothesize that AgNPs could be interacting with α_1

receptors in the rat heart as well and then blocking the Phe actions. Other reports have demonstrated that AgNPs significantly inhibited or reduced the ACh-induced NO-mediated vasodilation (8, 12); hence, these NMs may be interfering with ACh vasoactive and cardiac effects in the same way in our model. Indeed, after treatment with 100 $\mu\text{g}/\text{mL}$ AgNPs only, we detected NPs-derived silver within cardiac muscle, suggesting that AgNPs may be retained in the tissue and possibly interacting with Phe and ACh receptors and some stages of their signaling pathways, hindering their classic cardiac actions. Although we only identified silver at 100 $\mu\text{g}/\text{mL}$ AgNPs, we do not hesitate that there would be retained silver with lower concentrations, but the technique detection limit that ranges in microscopic scale, did not allow us to detect it. Furthermore, since we found that 10 and 100 $\mu\text{g}/\text{mL}$ AgNPs promoted severe damage to the heart at tissue level and considering that AgNPs-induced cardiotoxicity has been observed at concentrations starting at 100 $\mu\text{g}/\text{mL}$ and higher (13), we do not discard that AgNPs-induced damage in cardiomyocytes could impair cardiac contractility in response to subsequent Phe and ACh administrations. We also demonstrated, as in previous studies (8, 55, 56), that AgNPs effects are attributable to its nanometer size, since AgBMs did not modify cardiac parameters, NO production, MDA generation nor protein expression. Likewise, AgNO_3 did not change cardiac parameters, MDA generation nor protein expression, but increased NO at the same concentrations that AgNPs did, for this reason, we believe that AgNPs may involve Ag ionic processes in NO production but not in cardiac effects. One common point for AgNPs, AgBMs and AgNO_3 is that all treatments interfered with Phe and ACh effects. For the AgBMs case, it may be due to because of their micrometer size, they probably became trapped within the coronary vessels as it was reported for micro-sized particles intravenously administered directly into pulmonary arterioles from Broiler chickens (57), that in turn could be generating a stearic

hindrance between Phe and ACh with their receptors, blocking their effects. Regarding to AgNO₃, considering its cardiotoxicity (13), we suggest that both Phe and ACh do not exert their classic actions on isolated rat hearts, because of the loss of viability of cardiomyocytes. However, these effects have not been completely elucidated.

It is important to mention that AgNPs effects we have shown in this work on isolated perfused rat hearts were reached at high and unrealistic concentrations in comparison to those found in the environment as well as in cardiac tissue after dermal, oral, ingested and inhaled exposure (3). However, it must be taken into account, firstly that our results support the observations from epidemiological studies that NPs exposure may affect heart rhythm, heart rate variability and cardiac morbidity (5, 58). Secondly, most of the studies focused on the evaluation of AgNPs toxicity, both *in vivo* and *in vitro*, have used the same or even higher doses; moreover, several AgNPs-containing consumer products could lose nearly 100% of its total AgNPs content (2) reaching levels up to 500 µg of Ag (59).

In conclusion, the present study shows that AgNPs induce direct effects on cardiac physiology through NO generation and OS. Further investigations are required in order to elucidate the signaling pathway involved in these events. We also join to present and advocate the isolated and perfused rat heart Langendorff preparation as a suitable method to evaluate the NMs impact on cardiac physiology and then understand their mechanisms of action (17). This model allows to study the organ in isolation through continuous monitoring of the cardiac physiology in response to different kind of agents perfused into the heart, which guarantees the direct exposure of whole tissue to the treatment under study, reducing the influence of other organ systems and exocrine control that may confound physiological measurements (23, 60). Therefore, the Langendorff model may serve as a reference for other studies about chronic or

acute effects of AgNPs through different routes of exposure. Furthermore, biochemical analysis of the venous effluent as well as of the cardiac tissue, provides substantial information at the molecular, cellular and tissue levels, allowing its association with the physiological events observed, and therefore, a more adequate and accurate interpretation of the data.

ACCEPTED MANUSCRIPT

REFERENCES

1. Fiorino DJ. Voluntary Initiatives, Regulation, and Nanotechnology Oversight: Charting a Path. Project on Emerging Nanotechnologies Publication 19. 2010.
2. Yu S-j, Yin Y-g, Liu J-f. Silver nanoparticles in the environment. *Environmental Science: Processes & Impacts*. 2013;15(1):78-92.
3. Bachler G, von Goetz N, Hungerbühler K. A physiologically based pharmacokinetic model for ionic silver and silver nanoparticles. *Int J Nanomedicine*. 2013;8:3365-82.
4. Gonzalez C, Rosas-Hernandez H, Ramirez-Lee MA, Salazar-Garcia S, Ali SF. Role of silver nanoparticles (AgNPs) on the cardiovascular system. *Arch Toxicol*. 2016;90(3):493-511.
5. Schulz H, Harder V, Ibald-Mulli A, Khandoga A, Koenig W, Krombach F, et al. Cardiovascular effects of fine and ultrafine particles. *Journal of aerosol medicine : the official journal of the International Society for Aerosols in Medicine*. 2005;18(1):1-22.
6. Rastaldo R, Pagliaro P, Cappello S, Penna C, Mancardi D, Westerhof N, et al. Nitric oxide and cardiac function. *Life sciences*. 2007;81(10):779-93.
7. Zhao Y, Vanhoutte PM, Leung SWS. Vascular nitric oxide: Beyond eNOS. *Journal of Pharmacological Sciences*. 2015;129(2):83-94.
8. Rosas-Hernandez H, Jimenez-Badillo S, Martinez-Cuevas PP, Gracia-Espino E, Terrones H, Terrones M, et al. Effects of 45-nm silver nanoparticles on coronary endothelial cells and isolated rat aortic rings. *Toxicol Lett*. 2009;191(2-3):305-13.

9. Raieszadeh H, Noaman V, Yadegari M. Echocardiographic Assessment of Cardiac Structural and Functional Indices in Broiler Chickens Treated with Silver Nanoparticles. *The Scientific World Journal*. 2013;2013.
10. Asharani P, Wu YL, Gong Z, Valiyaveetil S. Toxicity of silver nanoparticles in zebrafish models. *Nanotechnology*. 2008;19(25):255102.
11. Chies AB, de Oliveira AM, Pereira FC, de Andrade CR, Correa FM. Phenylephrine-induced vasoconstriction of the rat superior mesenteric artery is decreased after repeated swimming. *J Smooth Muscle Res*. 2004;40(6):249-58.
12. Roberts JR, McKinney W, Kan H, Krajnak K, Frazer DG, Thomas TA, et al. Pulmonary and cardiovascular responses of rats to inhalation of silver nanoparticles. *J Toxicol Environ Health A*. 2013;76(11):651-68.
13. Korani M, Rezayat SM, Arbabi Bidgoli S. Sub-chronic Dermal Toxicity of Silver Nanoparticles in Guinea Pig: Special Emphasis to Heart, Bone and Kidney Toxicities. *Iran J Pharm Res*. 2013;12(3):511-9.
14. Bostan HB, Rezaee R, Valokala MG, Tsarouhas K, Golokhvast K, Tsatsakis AM, et al. Cardiotoxicity of nano-particles. *Life Sci*. 2016.
15. Taju G, Abdul Majeed S, Nambi KSN, Sahul Hameed AS. In vitro assay for the toxicity of silver nanoparticles using heart and gill cell lines of *Catla catla* and gill cell line of *Labeo rohita*. *Comparative Biochemistry and Physiology Part C: Toxicology & Pharmacology*. 2014;161:41-52.
16. Ebabe Elle R, Gaillet S, Vide J, Romain C, Lauret C, Rugani N, et al. Dietary exposure to silver nanoparticles in Sprague-Dawley rats: effects on oxidative stress and inflammation. *Food Chem Toxicol*. 2013;60:297-301.

17. Stampfl A, Maier M, Radykewicz R, Reitmeir P, Gottlicher M, Niessner R. Langendorff heart: a model system to study cardiovascular effects of engineered nanoparticles. *ACS Nano*. 2011;5(7):5345-53.
18. Yu X, Hong F, Zhang YQ. Bio-effect of nanoparticles in the cardiovascular system. *Journal of biomedical materials research Part A*. 2016;104(11):2881-97.
19. Espinosa-Cristobal LF, Martinez-Castañon GA, Loyola-Rodriguez JP, Patiño-Marin N, Reyes-Macías JF, Vargas-Morales JM, et al. Toxicity, distribution, and accumulation of silver nanoparticles in Wistar rats. *J Nanopart Res*. 2013;15(6):1-12.
20. Li Y, Yang Q, Li M, Song Y. Rate-dependent interface capture beyond the coffee-ring effect. *Scientific Reports*. 2016;6:24628.
21. Herrera-Gomez MB-S, O. Ceballos-Sanchez and M. O. Vazquez-Lepe. Practical methods for background subtraction in photoemission spectra: *Surf. Interface Anal.*; 2014, 46, 897–905.
22. Herrera-Gomez A. A double Lorentzian shape for asymmetric photoelectron peaks Internal report; 2011, CINVESTAV- Queretaro
23. Skrzypiec-Spring M, Grotthus B, Szelag A, Schulz R. Isolated heart perfusion according to Langendorff---still viable in the new millennium. *J Pharmacol Toxicol Methods*. 2007;55(2):113-26.
24. Gonzalez C, Corbacho AM, Eiserich JP, Garcia C, Lopez-Barrera F, Morales-Tlalpan V, et al. 16K-prolactin inhibits activation of endothelial nitric oxide synthase, intracellular calcium mobilization, and endothelium-dependent vasorelaxation. *Endocrinology*. 2004;145(12):5714-22.

25. Mahmood T, Yang PC. Western Blot: Technique, Theory, and Trouble Shooting. North American Journal of Medical Sciences. 2012;4(9):429-34.
26. Bryan NS, Grisham MB. Methods to detect nitric oxide and its metabolites in biological samples. Free Radic Biol Med. 2007;43(5):645-57.
27. Miranda KM, Espey MG, Wink DA. A rapid, simple spectrophotometric method for simultaneous detection of nitrate and nitrite. Nitric Oxide. 2001;5(1):62-71.
28. Ohkawa H, Ohishi N, Yagi K. Assay for lipid peroxides in animal tissues by thiobarbituric acid reaction. Analytical biochemistry. 1979;95(2):351-8.
29. van Essen HF, Verdaasdonk MA, Elshof SM, de Weger RA, van Diest PJ. Alcohol based tissue fixation as an alternative for formaldehyde: influence on immunohistochemistry. Journal of clinical pathology. 2010;63(12):1090-4.
30. Ding BA, Pirone A, Lenzi C, Xiaoming N, Baglini A, Romboli I. Histochemical features of the Muscovy duck small intestine during development. Tissue and Cell. 2011;43(3):190-5.
31. Meléndrez MF, Cárdenas G, Arbiol J. Synthesis and characterization of gallium colloidal nanoparticles. Journal of Colloid and Interface Science. 2010;346(2):279-87.
32. John F. Moulder WFS, Peter E. Sobol, and Keneth D. Bomben. Handbook of X-ray Photoelectron Spectroscopy. Japan.: Physical Electronics Inc. ; 1992.
33. Vassallo PF, Stefanon I, Rossoni LV, Tucci PJ, Vassallo DV. The left ventricular contractility of the rat heart is modulated by changes in flow and alpha 1-adrenoceptor stimulation. Brazilian journal of medical and biological research = Revista brasileira de pesquisas medicas e biologicas / Sociedade Brasileira de Biofisica [et al]. 1998;31(10):1353-9.

34. Takahashi H, Maehara K, Onuki N, Saito T, Maruyama Y. Decreased contractility of the left ventricle is induced by the neurotransmitter acetylcholine, but not by vagal stimulation in rats. *Japanese heart journal*. 2003;44(2):257-70.
35. Quyyumi AA, Dakak N, Andrews NP, Gilligan DM, Panza JA, Cannon RO. Contribution of Nitric Oxide to Metabolic Coronary Vasodilation in the Human Heart. *Circulation*. 1995;92(3):320-6.
36. Kim D-Y, Suk Sung J, Kim M, Ghodake G. Rapid production of silver nanoparticles at large-scale using gallic acid and their antibacterial assessment. *Materials Letters*. 2015;155:62-4.
37. Razavian MH, Masaimanesh M. Ingestion of silver nanoparticles leads to changes in blood parameters. *Nanomedicine Journal*. 2014;1(5):339-45.
38. Kojda G, Kottenberg K. Regulation of basal myocardial function by NO. *Cardiovascular research*. 1999;41(3):514-23.
39. Lodish H, Berk A, Zipursky SL, Matsudaira P, Baltimore D, Darnell J. *Muscle: A Specialized Contractile Machine*. 2000.
40. Albanese A, Tang PS, Chan WC. The effect of nanoparticle size, shape, and surface chemistry on biological systems. *Annual review of biomedical engineering*. 2012;14:1-16.
41. Müller-Strahl G, Kottenberg K, Zimmer HG, Noack E, Kojda G. Inhibition of nitric oxide synthase augments the positive inotropic effect of nitric oxide donors in the rat heart. *The Journal of Physiology*. 2000;522(Pt 2):311-20.
42. Chen Y, Traverse JH, Du R, Hou M, Bache RJ. Nitric oxide modulates myocardial oxygen consumption in the failing heart. *Circulation*. 2002;106(2):273-9.
43. Marnett LJ. Lipid peroxidation-DNA damage by malondialdehyde. *Mutation research*. 1999;424(1-2):83-95.

44. van der Loo B, Bachschmid M, Labugger R, Schildknecht S, Kilo J, Hahn R, et al. Expression and activity patterns of nitric oxide synthases and antioxidant enzymes reveal a substantial heterogeneity between cardiac and vascular aging in the rat. *Biogerontology*. 2005;6(5):325-34.
45. Kohen R, Nyska A. Oxidation of biological systems: oxidative stress phenomena, antioxidants, redox reactions, and methods for their quantification. *Toxicol Pathol*. 2002;30(6):620-50.
46. Choi JE, Kim S, Ahn JH, Youn P, Kang JS, Park K, et al. Induction of oxidative stress and apoptosis by silver nanoparticles in the liver of adult zebrafish. *Aquatic toxicology* (Amsterdam, Netherlands). 2010;100(2):151-9.
47. Adeyemi OS, Faniyan TO. Antioxidant status of rats administered silver nanoparticles orally. *Journal of Taibah University Medical Sciences*. 2014;9(3):182-6.
48. Valko M, Leibfritz D, Moncol J, Cronin MT, Mazur M, Telser J. Free radicals and antioxidants in normal physiological functions and human disease. *Int J Biochem Cell Biol*. 2007;39(1):44-84.
49. Hunter JD, Gregg K, Damani Z. Rhabdomyolysis. *Continuing Education in Anaesthesia, Critical Care & Pain*. 2006;6(4):141-3.
50. Torres PA, Helmstetter JA, Kaye AM, Kaye AD. Rhabdomyolysis: pathogenesis, diagnosis, and treatment. *The Ochsner journal*. 2015;15(1):58-69.
51. Al-Ismaili Z, Piccioni M, Zappitelli M. Rhabdomyolysis: pathogenesis of renal injury and management. *Pediatric Nephrology*. 2011;26(10):1781-8.
52. Vanholder R, SEVER MS, Ereğ E, Lameire N. Rhabdomyolysis. *Journal of the American Society of Nephrology*. 2000;11(8):1553-61.

53. Kennedy DC, Tay L-L, Lyn RK, Rouleau Y, Hulse J, Pezacki JP. Nanoscale aggregation of cellular β 2-adrenergic receptors measured by plasmonic interactions of functionalized nanoparticles. *ACS nano*. 2009;3(8):2329-39.
54. Torp KD, Tschakovsky ME, Halliwill JR, Minson CT, Joyner MJ. beta-Receptor agonist activity of phenylephrine in the human forearm. *J Appl Physiol* (1985). 2001;90(5):1855-9.
55. Ramirez-Lee MA, Rosas-Hernandez H, Salazar-Garcia S, Gutierrez-Hernandez JM, Espinosa-Tanguma R, Gonzalez FJ, et al. Silver nanoparticles induce anti-proliferative effects on airway smooth muscle cells. Role of nitric oxide and muscarinic receptor signaling pathway. *Toxicol Lett*. 2014;224(2):246-56.
56. Gonzalez C, Salazar-Garcia S, Palestino G, Martinez-Cuevas PP, Ramirez-Lee MA, Jurado-Manzano BB, et al. Effect of 45 nm silver nanoparticles (AgNPs) upon the smooth muscle of rat trachea: role of nitric oxide. *Toxicol Lett*. 2011;207(3):306-13.
57. Wideman RF, Jr., Erf GF. Intravenous micro-particle injection and pulmonary hypertension in broiler chickens: cardio-pulmonary hemodynamic responses. *Poultry science*. 2002;81(6):877-86.
58. Pieters N, Koppen G, Van Poppel M, De Prins S, Cox B, Dons E, et al. Blood Pressure and Same-Day Exposure to Air Pollution at School: Associations with Nano-Sized to Coarse PM in Children. *Environ Health Perspect*. 2015;123(7):737-42.
59. Benn TM, Westerhoff P. Nanoparticle silver released into water from commercially available sock fabrics. *Environmental science & technology*. 2008;42(11):4133-9.
60. Bell RM, Mocanu MM, Yellon DM. Retrograde heart perfusion: the Langendorff technique of isolated heart perfusion. *J Mol Cell Cardiol*. 2011;50(6):940-50.

FIGURE LEGENDS**Figure 1. AgNPs and AgBMs characterization.**

TEM micrograph showing pseudo-spherical AgNPs dispersed (A). SEM micrograph showing irregular shapes of AgBMs in micrometer sizes (B). Size distribution by number obtained by DLS analysis (C).

Figure 2. XPS spectra of gallic acid-synthesized AgNPs. X-ray photoelectron spectra of AgNPs (A), pure metallic Ag (silver foil 99.99%) (B) and Ag standard spectra from XPS Handbook (C).

Figure 3. Effects induced by AgNPs in coronary vascular tone and cardiac contractility in perfused rat hearts.

PP and LVP were taken as an index of coronary vascular tone and cardiac contractility, respectively. Values were recorded in millimeters of mercury (mmHg) from isolated perfused rat hearts in Langendorff preparation. PP (A) and LVP (B) representative trace recordings in response to 10 μ M Phe and 10 μ M ACh. PP (C) and LVP (D) representative trace recordings in response to consecutive administrations of increasing concentrations of AgNPs (0.1, 1, 10 and 100 μ g/mL), followed by 10 μ M Phe and 10 μ M ACh administrations. Results are expressed as % of control PP (E) and LVP (F) (n=5 animals). Data were analyzed with Kruskal-Wallis test in E; *p<0.005 vs control.

Figure 4. AgNPs induced iNOS-derived NO production and increased MDA levels in rat cardiac tissue.

NO₂/NO₃ was measured as an index for NO production in venous effluent in response to 10 μM Phe and 10 μM ACh as well as to increasing concentrations of AgNPs (0.1, 1, 10 and 100 μg/mL) and the following 10 μM Phe and 10 μM ACh treatments (A). Data were analyzed using the Kruskal-Wallis test; *p<0.005 vs control. MDA generation was quantified as an index of oxidative stress in response to increasing concentrations of AgNPs (0.1, 1, 10 and 100 μg/mL) (B). Western blot analysis was performed from homogenized hearts. eNOS, iNOS, CAT and SOD were detected at 140, 130, 64 and 23 kDa, respectively (C). Protein expression was normalized to glyceraldehydes-3-phosphate dehydrogenase (GAPDH) (D). Data were analyzed using one-way ANOVA; *p<0.05, **p<0.01 and ***p<0.001 vs control.

Figure 5. Effects of AgNPs in cardiac tissue.

Microphotographs of rat cardiac tissue. Control shows endocardium with normal cardiomyocytes (A and F). 0.1 μg/mL AgNPs treated heart showed cellular tumefaction and myofibrillar (*) and nucleus degeneration (**) (B). Vacuolization (*) was observed; however, striations are preserved as observed in augmented image (G). 1 μg/mL AgNPs treated heart showed cell atrophy, myofibrillar degeneration (*), tumefaction and nucleus degeneration (C). Nucleus degeneration (*) was observed as well as a slightly loss of transversal striations as observed in augmented image (H). 10 μg/mL AgNPs treated heart showed abnormalities including necrosis (○), cellular vacuolization (*), sarcoplasmic retractions (**), karyorrhexis (+) and rhabdomyolysis (D and I). 100 μg/mL AgNPs treated heart also showed abnormalities like cellular vacuolization (*), necrosis, degradation and fragmentation of nucleus, karyorrhexis and rhabdomyolysis (E and J). Microphotographs of rat cardiac tissue stained with Grimelius technique. Control shows normal

cardiomyocytes with no silver clusters (K). Positive control tissue from appendix carcinoid tumor showing silver clusters (*) as brown spots (L). 100 µg/mL AgNPs treated heart showing silver clusters located within the myocardium, specifically in the sarcoplasm (*) (M). Bars=10 µm.

Figure 6. Effect of AgBMs and AgNO₃ in coronary vascular tone, cardiac contractility and NO production of perfused rat hearts.

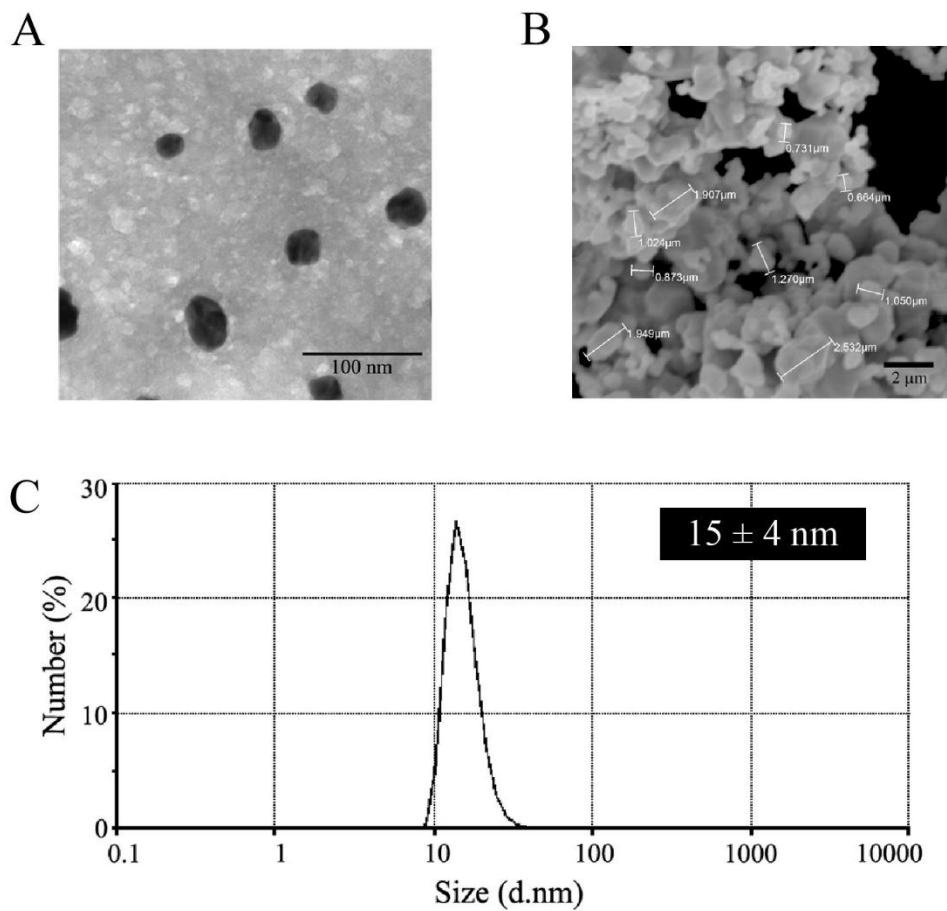
PP and LVP were taken as an index of coronary vascular tone and cardiac contractility, respectively. Values were recorded in millimeters of mercury (mmHg) from isolated perfused rat hearts in Langendorff preparation. PP and LVP results are expressed as % of control (n=5 animals) in response to 10 µM Phe and 10 µM ACh, cumulative administrations of (0.1, 1, 10 and 100 µg/mL) of AgBMs (A and C) and AgNO₃ (B and D) followed by 10 µM Phe and 10 µM ACh administrations. NO production in venous effluent in response to 10 µM Phe and 10 µM ACh, increasing concentrations of AgBMs (E) and AgNO₃ (F) (0.1, 1, 10 and 100 µg/mL) and their following 10 µM Phe and 10 µM ACh treatments. In A and C, a one-way ANOVA was performed to analyze the data; *p<0.05 and **p<0.01 vs control. In B, D and E data were analyzed with Kruskal-Wallis test; *p<0.005 vs control.

Figure 7. AgBMs and AgNO₃ do not modify MDA levels nor protein expression in rat cardiac tissue.

Rat hearts were treated with cumulative concentrations AgBMs and AgNO₃ (from 0.1 to 100 µg/mL). MDA generation was quantified as an index of oxidative stress (A). Presence of eNOS, iNOS, CAT and SOD was detected at 140, 130, 64 and 23 kDa, respectively (B). Protein expression normalized to GAPDH (C).

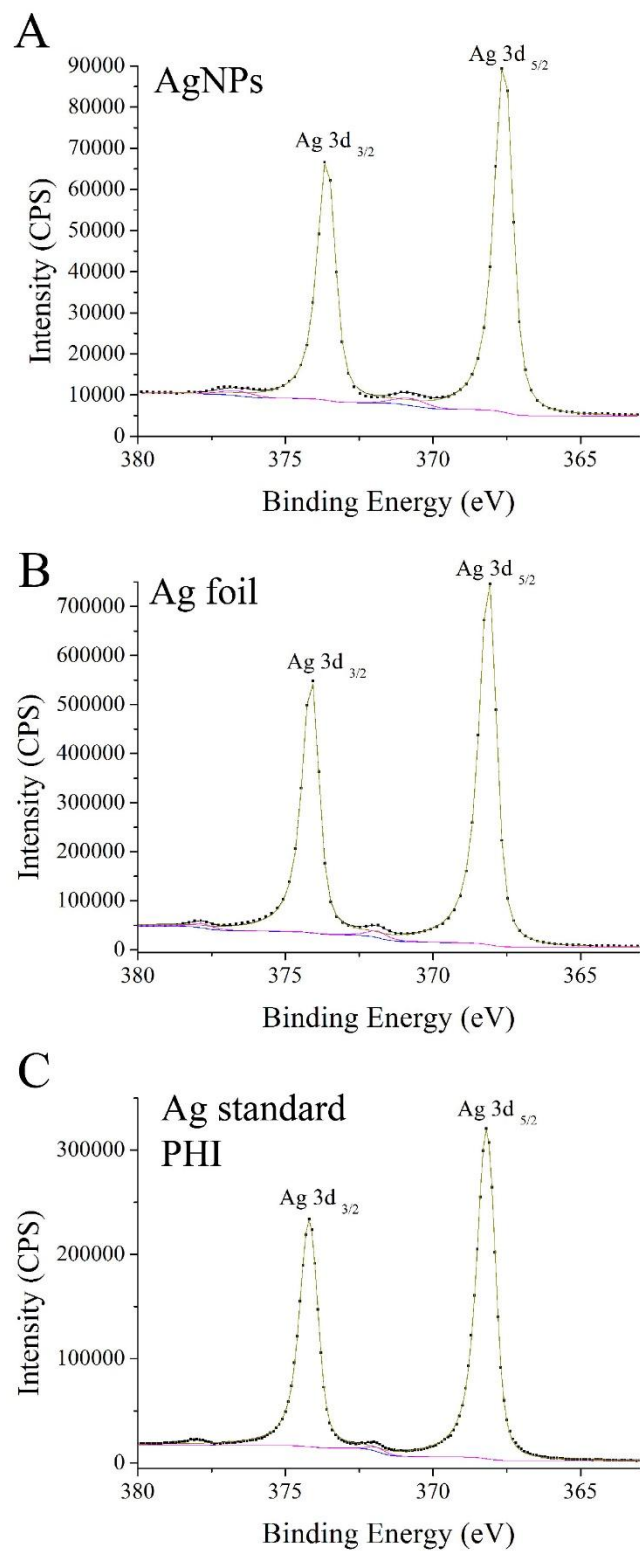
FIGURES

Figure 1.



A

Figure 2.



SCRIPT

Figure 3.

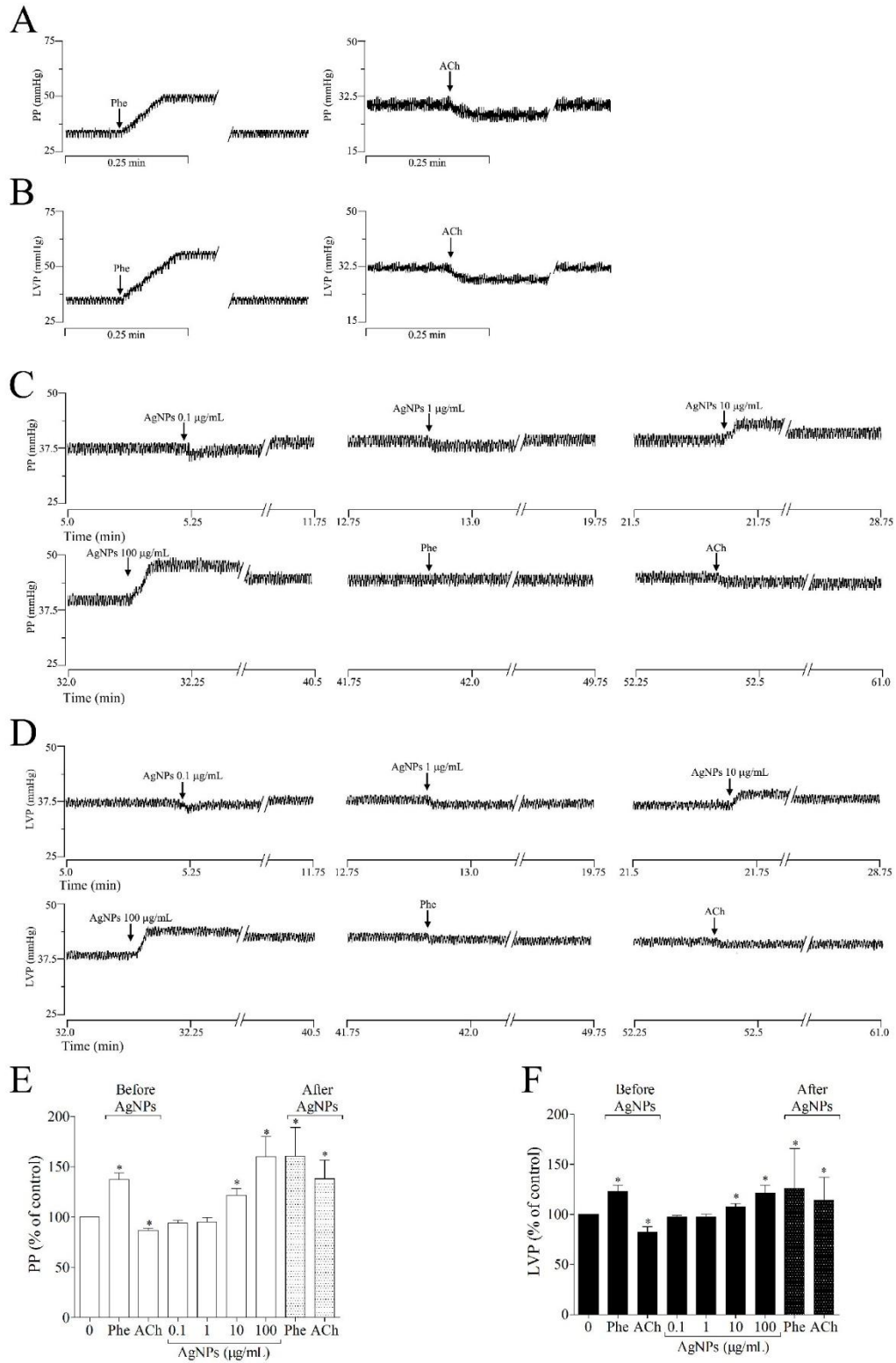
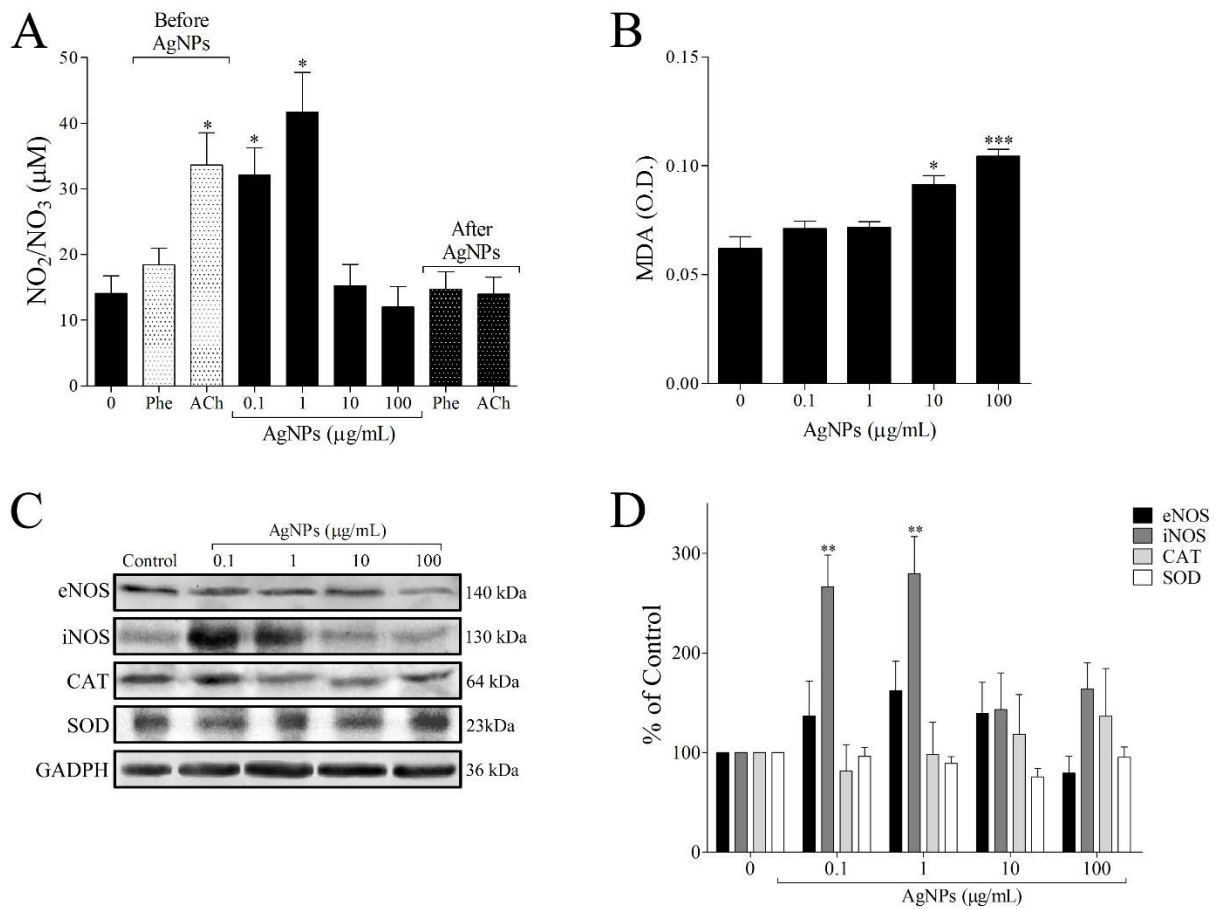


Figure 4.



ACQ

Figure 5.

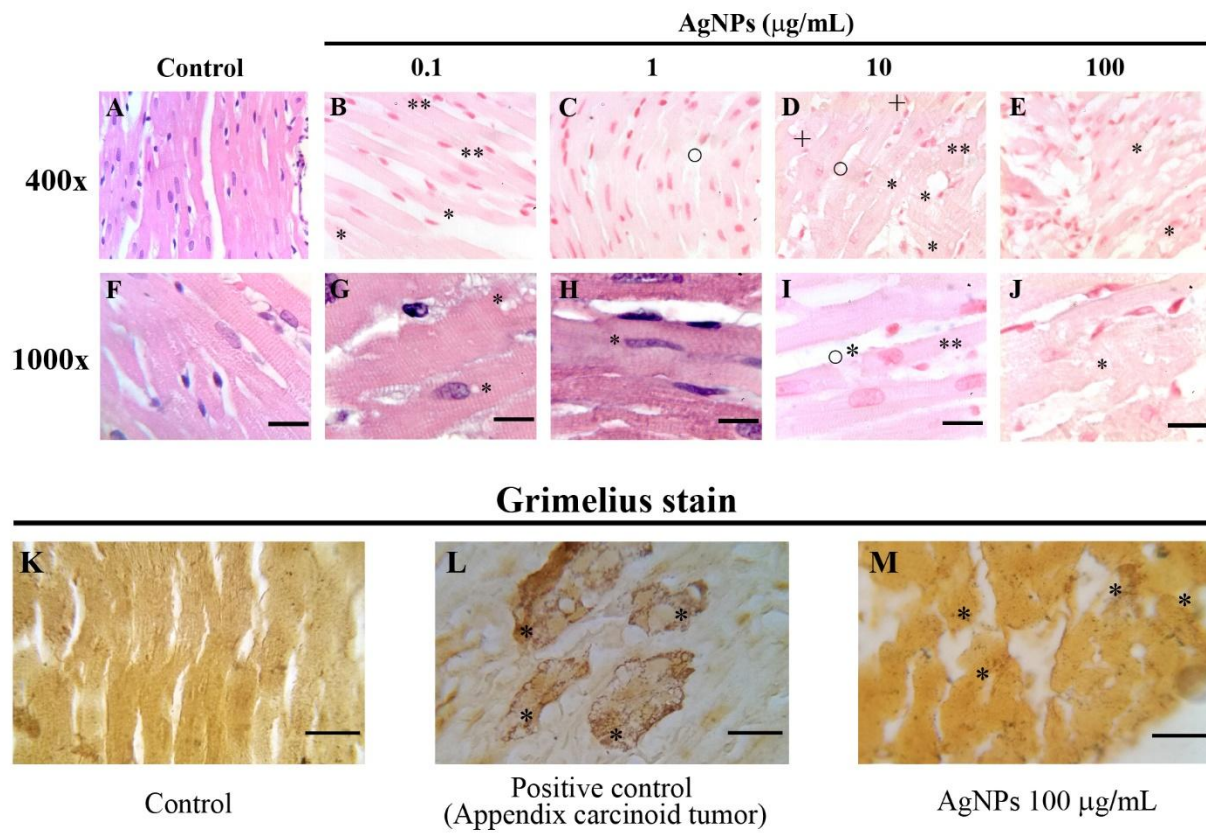


Figure 6.

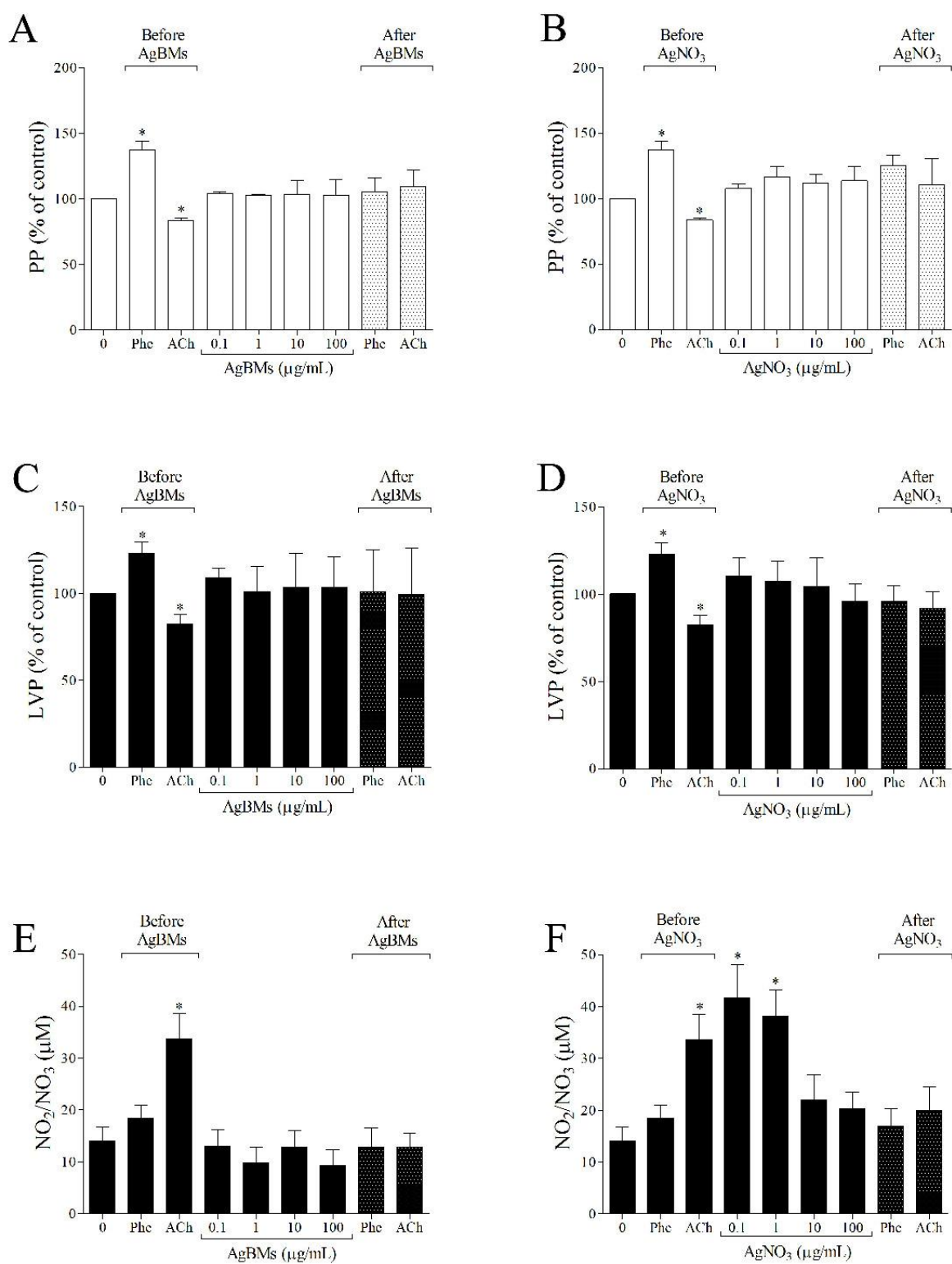
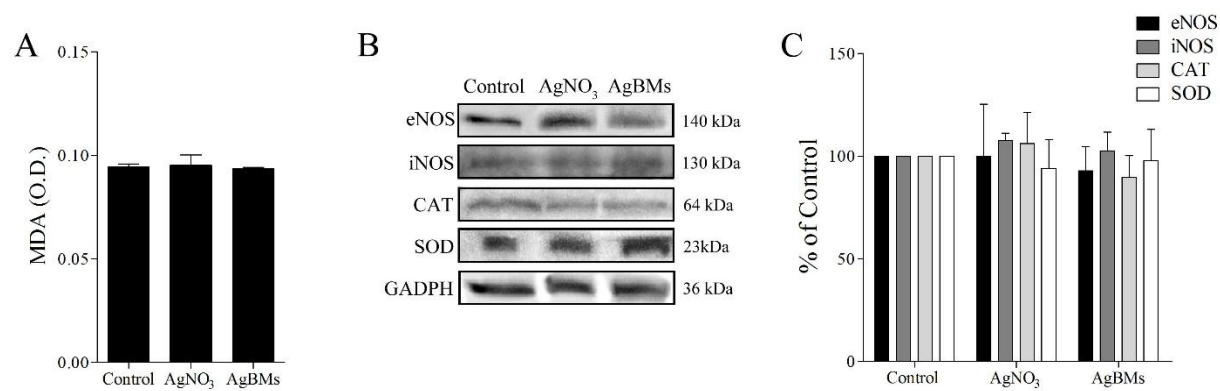
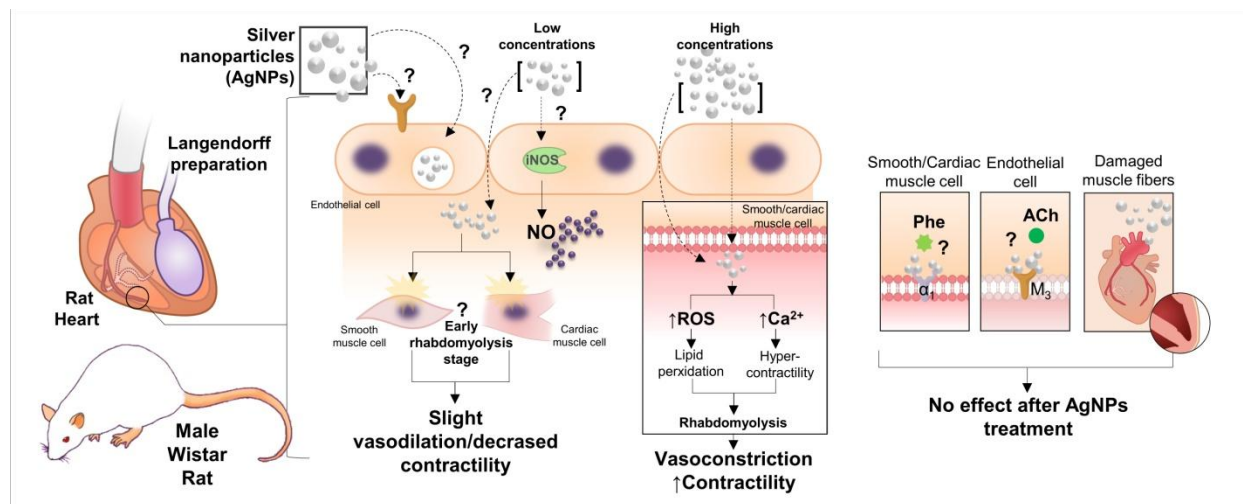


Figure 7.



ACCEPTED MANUSCRIPT



GRAPHICAL ABSTRACT TEXT

Silver nanoparticles (AgNPs) cardiac effects were evaluated using the Langendorff rat heart preparation. At low concentrations, AgNPs increased nitric oxide (NO) derived from inducible NO synthase (iNOS), without modifying coronary vascular tone nor cardiac contractility. Meanwhile, high concentrations induced a sustained vasoconstriction and increased cardiac contractility related to increased reactive oxygen species (ROS) levels, leading the triggering of rhabdomyolysis, which is the degradation of muscle. Furthermore, AgNPs were able to internalize to cardiac muscle cells, hindering the well-known actions induced by vasoactive controls phenylephrine (Phe) and acetylcholine (ACh). Future approaches are needed to elucidate the mechanism of action involved.